



# Colorimetric point-of-care paper-based sensors for urinary creatinine with smartphone readout

Izabela Lewińska<sup>a,\*</sup>, Mikołaj Speichert<sup>b</sup>, Mateusz Granica<sup>a</sup>, Łukasz Tymecki<sup>a</sup>

<sup>a</sup> University of Warsaw, Faculty of Chemistry, Pasteura 1, 02-093 Warsaw, Poland

<sup>b</sup> Gdansk University of Technology, Faculty of Electronics, Telecommunications and Informatics, Narutowicza 11/12, 80-233 Gdansk, Poland

## ARTICLE INFO

### Keywords:

Creatinine  
Jaffé  
3,5-dinitrobenzoic acid  
Microfluidic paper-based device  
Smartphone  
Computer vision

## ABSTRACT

Creatinine is a clinically significant analyte used to diagnose kidney condition. However, the literature still lacks in creatinine sensors fulfilling point-of-care testing requirements. In this paper, we have developed colorimetric paper-based creatinine sensors adhering to point-of-care testing principles. The signal readout is accomplished with a smartphone modified with 3D-printed elements and processed with a self-written application comprising computer vision algorithm for automatic detection of the colored zone. Two colorimetric methods – routinely used Jaffé method and an alternative one with 3,5-dinitrobenzoic acid were both tested and compared. Hue channel intensity from HSV color space and green channel from RGB color space was used as the analytical signal in Jaffé and 3,5-dinitrobenzoate method, respectively. For both kinds of sensors the linear range of the response covered the range significant for urinary analysis, with precision, expressed as RSD, below 5%. Limit of quantification for Jaffé method was  $1.05 \text{ mmol}\cdot\text{L}^{-1}$  whereas it was  $0.82 \text{ mmol}\cdot\text{L}^{-1}$  for 3,5-dinitrobenzoate method. The utility of the developed sensors to selectively quantify creatinine in undiluted urine was proved using artificial urine samples and the obtained recoveries were in the range from 70 to 129 %.

## 1. Introduction

Even though point-of-care testing (PoCT) is not a new concept, it has gained significant interest in recent years. PoCT refers to performing diagnostic tests at the time and place of patients' care, i.e., at a doctor's office, in an ambulance, at the bedside in a hospital or even at patients' homes. The general requirements for point-of-care tests are: (i) can be performed by an unskilled user (user-friendly devices), (ii) short turnout time, (iii) minimal to no auxiliary equipment needed. As stated by Price [1], PoCT has significant economic benefits besides obviously improving clinical decision-making processes.

A platform for creating such tests, fully coherent with PoCT concepts, is paper, introduced into the modern analytical chemistry by the Whitesides group in 2007 [2]. Paper as solid support for analytical tests has numerous advantages. It is inexpensive, flat and lightweight, easily disposable, and enables "pumping" without external devices due to capillary forces. Ever since, paper has been willingly used as matrix for analytical assays in environmental, clinical or food analysis and its use has been reviewed recently by Fu and Wang [3].

Considering that chronic kidney disease affects nearly 10 % of the global population as well as is a significant risk factor for cardiovascular

diseases, its early diagnosis and monitoring is of great importance [4]. Kidney disease can be preliminarily screened by quantifying creatinine in the patient's urine. The physiological level of creatinine in urine varies from  $2.5$  to  $17 \text{ mmol}\cdot\text{L}^{-1}$ . The most commonly employed method for creatinine determination is the Jaffé reaction, which relies on an absorbing complex formation during the reaction of creatinine with picric acid. Recently, we optimized and applied for urinary creatinine quantification an alternative method, based on creatinine reaction with 3,5-dinitrobenzoic acid (DNBA) [5]. The technique was superior to Jaffé assay in terms of selectivity as well as lower toxicity of reagents.

Some attempts to create microfluidic paper-based analytical devices ( $\mu$ PADs) dedicated for the quantification of creatinine have already been proposed in the literature. Sittiwong and Unob were the first to determine urinary creatinine on a paper platform [6]. They used an anionic species to extract creatinine cation from a sample, followed by applying the Jaffé reagents (alkaline picrate). Rossini et al. developed a  $\mu$ PAD for simultaneous colorimetric determination of urinary creatinine and uric acid [7]. Tseng et al. [8] proposed the only non-enzymatic  $\mu$ PAD suitable for the quantification of creatinine in blood with an incorporated membrane for the separation of cells and fibrinogen from whole blood samples. However, they employed single-point Jaffé method for the

\* Corresponding author.

E-mail address: [i.lewinska@uw.edu.pl](mailto:i.lewinska@uw.edu.pl) (I. Lewińska).

<https://doi.org/10.1016/j.snb.2021.129915>

Received 18 January 2021; Received in revised form 15 March 2021; Accepted 2 April 2021

Available online 6 April 2021

0925-4005/© 2021 The Author(s).

Published by Elsevier B.V. This is an open access article under the CC BY-NC-ND license

(<http://creativecommons.org/licenses/by-nc-nd/4.0/>).

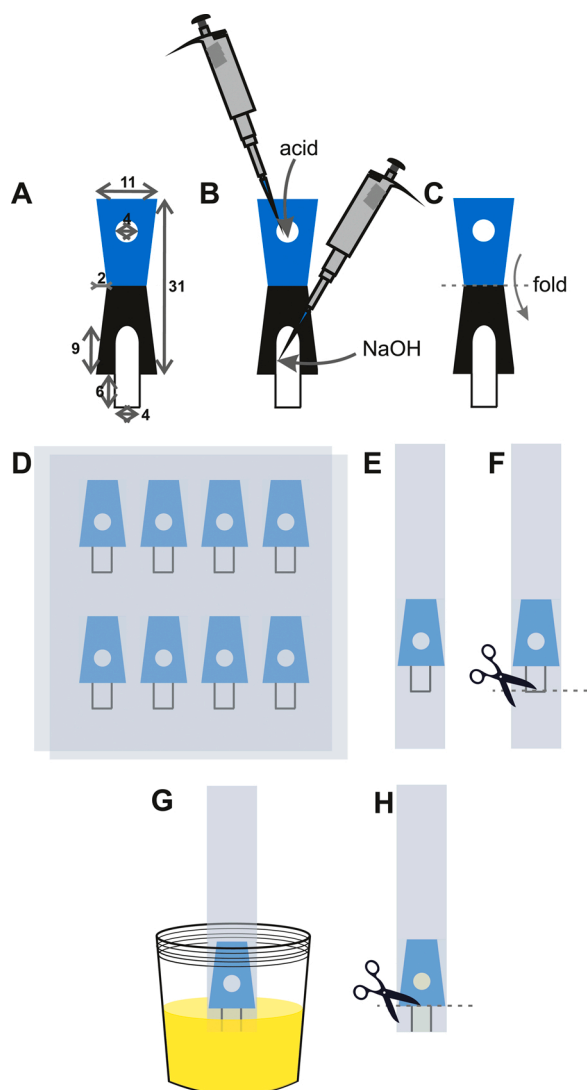


**Fig. 1.** The preparation of paper-based sensors and the analytical procedure. Refer to the text for detailed explanation of the steps.

determination of creatinine in serum, which is not recommended due to possible interferences from matrix components. Creatinine was also determined in the paper-based format using enzymatic [9–11] or electrochemical methods [12–14].

In this paper two colorimetric detection methods for paper-based creatinine sensors have been optimized and compared – the routinely used Jaffé method and a significantly safer to use alternative, a method with 3,5-dinitrobenzoic acid. The latter method was tested in paper-based sensors for the first time. Contrary to previous approaches, the urinary creatinine test can be performed with the aid of the developed sensors without any laboratory equipment such as micropipettes. The signal readout was accomplished with a smartphone modified with 3D-printed elements. Moreover, a computer vision algorithm was developed for automatic detection of the colored zone and was incorporated in a self-written application for signal acquisition and processing. The created platform, coherent with PoCT principles, was tested in real sensing scenarios.

## 2. Experimental section

### 2.1. Materials and instruments

Creatinine, 3,5-dinitrobenzoic acid (DNBA), picric acid (PA), bovine

serum albumin, citric acid, lactic acid, Whatman Filter Qualitative Filter Papers No. 1, 4 and 6 were obtained from Sigma Aldrich (USA). NaOH, urea, uric acid, methanol, NaCl,  $\text{NH}_4\text{Cl}$ ,  $\text{Na}_2\text{CO}_3$ ,  $\text{Na}_2\text{SO}_4$ ,  $\text{KH}_2\text{PO}_4$ ,  $\text{K}_2\text{HPO}_4$ ,  $\text{MgSO}_4$  and  $\text{CaCl}_2$  were purchased from Avantor Performance Materials (Poland). All reagents were used without further purification. Water used in all the experiments was passed through the HLP5 water purifying system (Hydrolab, Poland). Hot laminating films of 100  $\mu\text{m}$  thickness were used in a standard office laminator. Artificial urine composition is given in Electronic Supplementary Information [15].

### 2.2. Creatinine determination methods

Two colorimetric methods for the determination of creatinine were used – Jaffé and DNBA assays. They rely on an absorbing Janovsky complex formation when creatinine reacts with PA or DNBA (Fig. S1) in alkaline environment.

### 2.3. Sensors preparation

A ColorQube 8570 (Xerox, USA) solid ink printer was used to print out the desired shape and create hydrophobic barriers in the bulk paper. The architecture of the barriers was designed with the assistance of CorelDraw software (dimensions shown in Fig. 1, A). The printed paper was heated in a laboratory dried set to 120  $^\circ\text{C}$  for 2 min. This allowed the wax to melt and penetrate the pores in the paper. To prepare the sensors, an appropriate volume of reagents' solution was manually pipetted onto hydrophilic zones of the printed design and allowed to dry for about 15 min in the ambient conditions (Fig. 1, B). The sensors were then cut out, folded following the line between black and blue color (Fig. 1, C) and hot laminated (Fig. 1, D). The final stage was to cut out strips containing one paper-based device each (Fig. 1, E).

### 2.4. Analytical procedure

To conduct the creatinine quantification, the sensors were dipped in a way that only the bottom part of the sampler was immersed in the sample. Before the dipping process, the line at the end of the sensor was cut off to allow fluid flow through the sampler (Fig. 1, step F). The sensor was kept immersed in the solution until the sample reached the top of the sampling channel. Then the bottom part of the sampling channel was cut off with scissors and disposed of (Fig. 1, steps G and H). Such an approach prevents contamination of the case and smartphone with the sample. After an appropriate incubation time, the sensor was placed in the smartphone case and the photo was taken. Unless stated otherwise, each measurement was triplicated.

### 2.5. Smartphone modification and signal processing

For image acquisition, a smartphone (Samsung Galaxy A5, Samsung Electronics, South Korea) with a 13 MPx rear camera (Sony Exmor RS IMX135 CMOS sensor) was employed. Throughout the optimization experiments, the photos were recorded using OpenCamera v1.45.2 smartphone application (by Mark Harman). This application was chosen over the build-in one because it allows for selecting ISO parameter as well as white balance. Smartphone was modified with 3D printed elements; the design details are given in ESI (Fig. S2).

The obtained photos were transferred to the PC and analyzed using ImageJ software (National Institutes of Health, USA). A circular region of interest (ROI) was selected and applied to each of the taken photos. Then the RGB Measure function was used to obtain mean intensity of red, green and blue channel in the selected ROI. To obtain histograms, a Color Histogram plug-in was used. More details about the use of ImageJ software for photos processing are described in ESI. RGB color space was transformed to HSV color space using equations given in ESI.

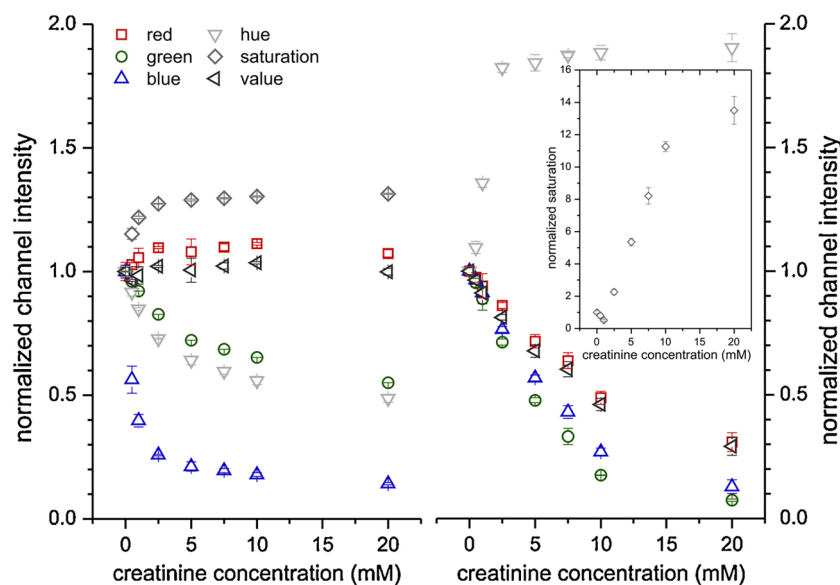


Fig. 2. Normalized calibration dependencies for (A): Jaffé-based sensors and (B): DNBA-based sensors for RGB and HSV color spaces. Insert: Calibration dependence of normalized saturation vs creatinine concentration for DNBA-based sensors.

## 2.6. Application development

A smartphone application was developed targeting Android operating system using state-of-the-art programming language named Kotlin, which is considered to be Java successor when it comes to Android development. Four main processes can be distinguished in the application flow: (1) taking a photo with disabled auto-exposure and auto white balance control routines and applied appropriate camera properties, like ISO and sensor exposure time; (2) determining positions of all non-black objects appearing in the photo; (3) analyzing the main non-black object and retrieving its average color scheme in RGB color space after pre-processing described below; (4) calculating creatinine concentration according to defined by the user slope and intercept of the calibration curve.

The non-black objects are determined using image segmentation algorithm [16] designed and written specifically for this problem. The calculation process begins with detecting the most frequently occurring color (background). The image pixels are being filtered by their color difference from the background determined by proximity threshold (an empirically defined value). The outcome pixels are being grouped using neighborhood-based clustering algorithm [17] and the biggest cluster is being chosen for the next operations. Before the process of color analysis, the cluster is brought to an ellipse and restrained by 30 % in order to limit the influence of boundary conditions. The color extracted from the calculated area is averaged and passed for further operations. The application is available for most modern Android phones with operating system versions higher than 5 as. APK file in the Supplementary Material.

## 3. Results and discussion

### 3.1. Architecture of the sensors

The key point in designing the architecture of the paper-based sensors working according to Jaffé or DNBA assay protocol is avoiding pre-mixing of the appropriate acid with the alkali. Such an approach results in a reaction between the reagents [18] and, therefore, changes in the sensors' sensitivity. For that reason, a double trapezoid shape was selected, which is shown in Fig. 1A. The two trapezoids have different colors to ease reproducible folding of the sensors. The shape of the sensors is trapezoidal instead of rectangular to avoid the laminating foil

unclinging. The lamination of the paper-based sensors serves several purposes: (i) it limits the influence of the ambient conditions on the pre-deposited reagents; (ii) it improves the mechanical properties (rigidity) of the sensors; (iii) it separates the user from a potentially contagious biological sample.

Several design choices had to be made to ensure the best possible analytical and practical parameters of the proposed sensors. First of all, three kinds of Whatman filter papers with various pore size (25  $\mu\text{m}$  – Grade 4, 11  $\mu\text{m}$  – Grade 1 and 3  $\mu\text{m}$  – Grade 6) were tested to establish which one provides fast and reproducible sampling. Among the chosen papers, Whatman Grade 6 did not promote vertical flow of fluid at all. The time needed for the sample to fill the sampling channel entirely was 55 s for Whatman Grade 4 paper and 120 s for Whatman Grade 1 paper. On the other hand, larger pore size contributed to washing out of the reagents deposited in the reaction zone. Considering the pros and cons, Grade 4 paper was selected for the manufacturing of sensors.

Since Jaffé reaction has already been studied in  $\mu\text{PADs}$ , it was selected as the model one and used to optimize the architecture of the sensors. The image acquisition can be performed from two sides of the paper-based devices – either with the reaction zone facing the camera or with the sampling channel facing the camera. These two approaches were compared in terms of sensitivity, linearity and precision. The precision was checked on two levels of creatinine concentration – 2.5 and 10  $\text{mmol}\cdot\text{L}^{-1}$ . The obtained RSD values for a sum of green and blue (the analytical signal used in Ref. [8]) channel ( $n = 6$ ) were 4.7 and 6.6 % for the detection from the sampling channel side and 5.2 and 8.2 % for the detection from the reaction zone side for lower and higher creatinine concentration, respectively. Moreover, the sensitivity, as well as the linear range, are superior in the former case therefore this mode of detection was selected for further experiments.

Another factor to consider is the width of the sampler and the diameter of the reaction zone. Three different widths/diameters were tested – 3, 4 and 5 mm. For 3 mm channel width, the diameter of the reaction zone was 3 mm and so on. The change in this parameter did not affect the analytical performance of the sensors significantly. However, the sensitivity and linearity of the sensors' response was superior for 4 mm width, as can be seen in Fig. S3, therefore this width was selected for further experiments. The length of the channel was not a subject of optimization because it was dictated by the dimensions of the smartphone case as well as practical considerations. The amount of sample consumed as well as precision of the sampling process was established

**Table 1**

The effect of change of selected parameters on the sensitivity and linearity of the developed paper-based sensors. Initial conditions were: [PA] = 40 mmol·L<sup>-1</sup>, [DNBA] = 0.3 mol·L<sup>-1</sup> in 0.45 mol·L<sup>-1</sup> NaOH, [NaOH] = 2 mol·L<sup>-1</sup>, ISO = 200.

Parameter to optimize	Parameter value	Jaffé-based sensors	
		Sensitivity*	R <sup>2</sup>
PA volume	1 µL	-15.4	0.975
	2 µL	-14.6	0.983
	2 µL	-18.7	0.979
NaOH volume	4 µL	-16.7	0.989
	6 µL	-17.6	0.990
	25 mM	-12.3	0.975
PA concentration	40 mM	-14.4	0.980
	55 mM	-16.0	0.989
	1 M	non linear	-
NaOH concentration	2 M	-19.0	0.956
	3 M	-9.61	0.984
	room temperature	-19.4	0.997
Incubation temperature	45 °C	-22.4	0.996
	60 °C	-22.5	0.997
	100	-25.2	0.999
	200	-18.7	0.997
ISO	400	-11.1	0.998
	800	-6.04	0.977
Parameter to optimize	Parameter value	DNBA-based sensors	
		Sensitivity**	R <sup>2</sup>
DNBA concentration	0.1 M (in 0.15 M NaOH)	-8.25	0.996
	0.2 M (in 0.3 M NaOH)	-13.6	0.983
	0.3 M (in 0.45 M NaOH)	-18.6	0.986
NaOH concentration	1 M	non linear	-
	2 M	-18.6	0.986
	3 M	-16.0	0.975
	room temperature	-19.4	0.960
Incubation temperature	45 °C	-9.36	0.988
	60 °C	-6.53	0.998
	100	-26.0	0.993
	200	-18.0	0.985
ISO	400	-17.8	0.984
	800	-7.60	0.966

\* sensitivity shown in hue intensity·(log(creatinine concentration [mM]))<sup>-1</sup>.

\*\* sensitivity shown in Green intensity·(creatinine concentration[mM])<sup>-1</sup>.

using gravimetric method. The estimated volume of the sample is 5.4 ± 0.5 µL (n = 15, RSD = 9.3 %). The imprecision of the sampling is attributed to the fact that the sampler is manually cut out. In the top part, adjacent to the detection zone, the amount of sample present should be much more reproducible, dictated mainly by the precision of the printer therefore it does not affect the obtained results significantly. In the Authors' opinion, this result is satisfactory for such a simple sampling system.

### 3.2. Color space selection

The choice of the color space, in which the obtained photos are analyzed, was made in the beginning. It is essential to highlight that sensors exploiting Jaffé reaction are bitonal, changing the color from yellow to orange, whereas sensors operating with DNBA method are monotonal. In the latter case, the color of the detection zone changes from white to purple in the course of the reaction.

The primary color space for photos in JPEG format is RGB model. At the same time, it is the most commonly used color space in digital color analysis as well as the only one used for image processing in paper-based sensors for creatinine present in the literature. Generally, it is preferable to work with unaltered RGB color space whenever it is possible. However, HSV color space can be advantageous in some cases. H (hue) channel provides all of the color information in a single parameter, which is especially beneficial for bitonal optical sensors. Moreover, it is supposed to provide superior precision and robustness to RGB color space [19]. For this reason, photos obtained for Jaffé and DNBA method

were analyzed in both color spaces to establish which channel should be chosen as the analytical signal. The obtained calibration curves in the range from 0 to 20 mmol·L<sup>-1</sup> of creatinine are shown in Fig. 2. The signals are normalized by dividing each value by the intensity obtained for the blank sample.

First of all, it is clear that the shape of the curves in both color spaces for Jaffé method is rather logarithmic than linear. For low creatinine concentrations, i.e. 0–2.5 mmol·L<sup>-1</sup> the most sensitive channel would be B from RGB color space. However, this range is not significant for urinary creatinine analysis. Both G and hue channels would provide similar sensitivity. To establish which of these channels shows superior precision histograms of R, G, B and hue channels were plotted and are shown in Fig. S4. Hue channel exhibits superior precision to any of RGB color space channels. Moreover, the coefficient of variation for 6 independent sensors for G and hue channel is 4.5 % and 3.6 %, respectively for 2.5 mmol·L<sup>-1</sup> of creatinine and 6.5 % and 3.0 %, respectively for 10 mmol·L<sup>-1</sup> of creatinine. Due to all the above-mentioned reasons, hue channel was chosen to be treated as the analytical signal for Jaffé-based sensors.

The picture is somewhat different for sensors based on reaction with DNBA. As they are monotonal, a linear decrease of each of RGB color space channel intensity is observed, with the green channel's change being the most profound. In HSV color space, a linear change of saturation and value parameters is expected for monotonal sensors [20]. The intensity of value channel corresponds to the most intense RGB channel (see equation 5 in ESI). Therefore, it provides similar sensitivity to R in the range of creatinine concentration significant for urinary analysis. In case of saturation channel, two linear ranges can be distinguished – from 0 to 1 mmol·L<sup>-1</sup> and from 1 to 10 mmol·L<sup>-1</sup>, as can be seen in insert in Fig. 2. Hue parameter does not change in the desired range. Bearing in mind that RGB color space is preferable because it does not require any mathematical conversions, G channel was selected as the optimal analytical signal.

### 3.3. Assays conditions optimization

The chemical, physical and instrumental conditions of the assay were optimized to find the ones providing the best sensitivity. The results of these experiments are summarized in Table 1. The chemical parameters to be optimized were the concentration of the appropriate acid and the concentration of sodium hydroxide. DNBA solutions were prepared in sodium hydroxide in molar ratio DNBA:NaOH equal to 1:1.5 [5]. In case of sensors relying on DNBA reaction with creatinine the washing out of the DNBA-based reagent by the sample was very significant (shown in photo in Fig. S5). Such problems are typically solved by depositing reagents in multiple steps. In fact, the washing out effect was diminished when DNBA reagent was deposited in 2 steps, but no further improvement was noticed more DNBA was applied. According to the literature [21], the volume of the deposited reagents strongly affects the magnitude of their displacement by the flowing sample. Multiple deposition steps translate into increased total volume of the deposited reagent and saturation of paper substrate. As a result, duplicate deposition of DNBA reagent were chosen to be applied in further experiments.

The optimal volume of both reagents was chosen basing on Jaffé sensors and used also in DNBA sensors. For the acid reagent 1 µL was chosen as the optimal and for NaOH solution 2 µL, deposited at the top of the sampling channel, was selected. In both cases, the largest of tested acid concentrations provided the best sensitivity of the sensors. Due to solubility issues, it was impossible to prepare aqueous PA and DNBA exceeding 55 mmol·L<sup>-1</sup> and 0.3 mol·L<sup>-1</sup>, respectively. 2 mol·L<sup>-1</sup> NaOH was chosen as the optimal one for both kind of sensors.

The influence of temperature on the response of the sensors was established next. In the literature, almost all Jaffé paper-based sensors require elevated temperature to initiate the reaction [7,8]. We found that elevating the temperature to 45 °C does in fact improve the sensitivity. Still, in the Authors' opinion, the change is not profound enough

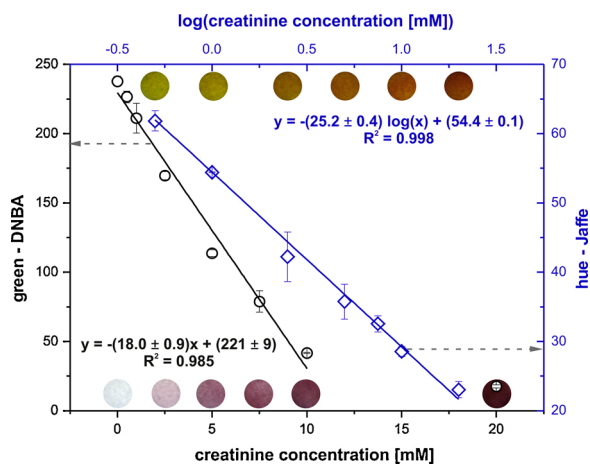


Fig. 3. Calibration curves for Jaffé- and DNBA-based sensors. The colorful spots are photos of the sensors' detection zones.

to justify the requirement for more instrumentation. For that reason, the sensors were incubated in ambient conditions. The influence of the temperature on the DNBA-based sensors is the opposite, the higher the temperature is, the lower the sensitivity. This is probably caused by an occurring side reaction, which results in a yellowish product, shown in photos in Fig. S6.

Last but not least, the ISO parameter of the camera was optimized. The ISO parameter is basically the sensitivity of the camera to the light. As shown in Table 1, the ISO setting significantly affects the calibration curve slope. Moreover, while the linear range of sensors based on Jaffé reaction is independent of ISO setting (Fig. S7), the linear range of

DNBA-based sensors strongly depends on the employed ISO parameter, as shown on calibration dependencies in Fig. S8. For ISO 100 the linear range is from 0 to 5 mmol·L<sup>-1</sup> of creatinine, for ISO 200 it is between 0 and 10 mmol·L<sup>-1</sup>, for ISO 400 from 1 to 10 mmol·L<sup>-1</sup> and for ISO 800 from 5 to 20 mmol·L<sup>-1</sup>. As a result, a change of ISO setting in the camera application can be used to easily alter the sensitivity as well as the linear range of the obtained sensors, without the need to change their chemical composition. The optimal ISO for Jaffé-based sensors was chosen to be 100, because of the highest sensitivity and 200 for DNBA-based sensors due to sufficient sensitivity and a wide linear range.

To establish the optimal incubation time, the kinetics of the reaction were registered for 1, 5 and 10 mmol·L<sup>-1</sup> of creatinine. The obtained results are presented in Fig. S9. For both methods the intensities decrease over time therefore the longer incubation time, the more sensitive detection. However, to limit the total analysis time, 6 min incubation (time measured from the moment of dipping the sensor in the sample) was selected for both kinds of sensors. To conclude this section, it is important to highlight that instead of one-variable-a-time approach, multivariate analysis could have been used to optimize the parameters as well as the architecture of the developed sensors [22].

The calibration curves obtained in the optimal conditions for both detection methods are shown in Fig. 3. The limits of detection and quantification were calculated basing on the following equations:  $LOD = 3.3SD_y/S$  and  $LOQ = 10SD_y/S$ , where  $S$  is the slope of the calibration curve and  $SD_y$  is the standard deviation of the intercept. For Jaffé-based sensors the estimated LOD and LOQ are 0.35 and 1.05 mmol·L<sup>-1</sup>, respectively. In case of the DNBA-based sensors the LOD is 0.27 mmol·L<sup>-1</sup> and the LOQ is 0.82 mmol·L<sup>-1</sup>. The precision, expressed as RSD of 6 independent sensors response for 5 mmol·L<sup>-1</sup> of creatinine, was found to be 4.4 % and 4.3 % for Jaffé-based and DNBA-based sensors, respectively.

Table 2

A comparison of selected colorimetric paper-based creatinine sensors with the developed ones. RT – room temperature, CAS is Chrome azurol S.

Method	Sample	Linear range [mmol·L <sup>-1</sup> ]	Analysis time	Temp.	Analytical signal	Detector	Ref.
Jaffé	whole blood	0.02 – 0.68	6 min	37 °C	G + B channel	CMOS camera	[8]
Jaffé	urine	0.46 – 5.31	12.5 min	elevated	G channel	scanner	[7]
Jaffé	urine	0.15 – 8.85	5 min	RT	R to G channel ratio	tablet camera	[24]
enzymatic	urine	0.22 – 2.21	7 min	RT	color intensity	scanner	[10]
CAS-Pd <sup>2+</sup>	urine	up to 26.5	15 min	RT	distance of colored zone	naked eye/ruler	[25]
Jaffé	urine	1.05 – 20.0	6 min	RT	hue channel	smartphone camera	this work
DNBA	urine	0.82 – 10.0	6 min	RT	G channel	smartphone camera	this work

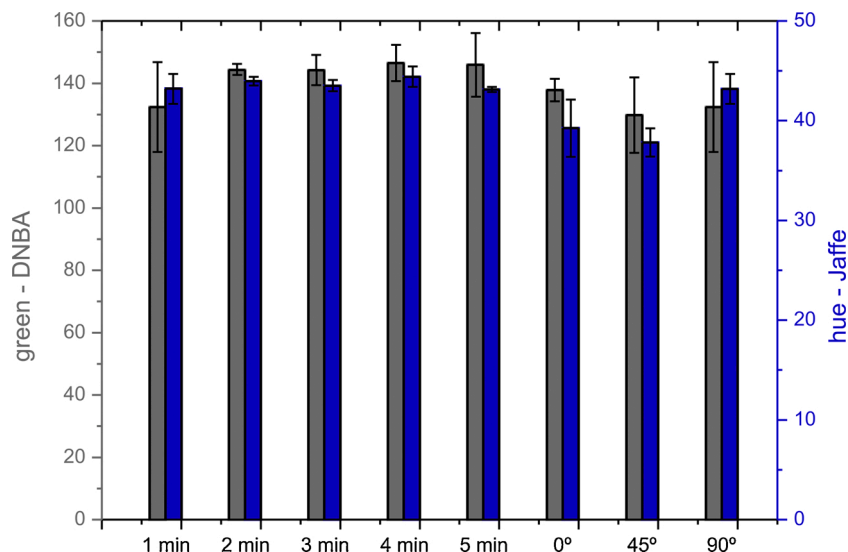
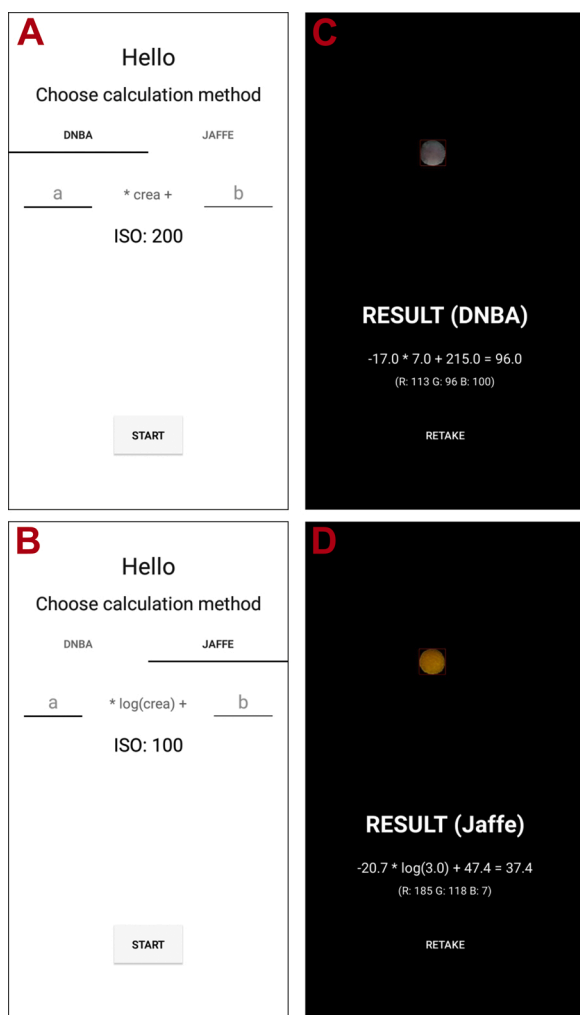


Fig. 4. The effect of the dipping time and the dipping angle on the sensors' response for Jaffé-based (hue parameter, right bars) and DNBA-based (green parameter, left bars) analytical devices.



**Fig. 5.** Application user flow: A, B – the starting screens for DNBA and Jaffé methods, respectively; C – screen with result for DNBA method, creatinine concentration was calculated with preset equation  $y = -17.0x + 215.0$  and the analytical signal is green channel intensity; D - screen with result for Jaffé method, creatinine concentration was calculated with preset equation  $y = -20.7 \log(x) + 47.4$  and the analytical signal is hue calculated from the measured R, G and B channel intensities.

The analytical performance of the obtained sensors was compared to those already reported in the literature and the comparison is presented in Table 2. The developed sensors do not stand out in terms of limit of quantification. However, the linear range of the sensors' response fits in the physiological range of creatinine in human urine, enabling the determination of this metabolite in undiluted urine samples. The linear range of DNBA-based sensors allows to determine creatinine in levels below and on the lower side of the physiological range, which is of great clinical significance. Low urinary creatinine is associated with higher mortality risk for patients with chronic kidney disease [23]. Moreover, the reported sensors are the only example of smartphone-assisted creatinine quantification. It is worth highlighting that smartphones, despite being excellently coherent with point-of-care testing principles, usually provide worse analytical parameters than traditional cameras.

### 3.4. Robustness, interferences and stability

Point-of-care sensors should be designed in a way so that they can be used by low-skilled users therefore the robustness of the proposed systems was tested. The influence of the dipping time as well as the dipping angle on the obtained results was established and is presented in Fig. 4.

As can be seen the dipping time does not significantly affect the response of the sensors basing on Jaffé reaction. In case of sensors with DNBA, above 2 min of dipping time the signal is also reasonably stable. However, the sensors' response is affected by the dipping angle, especially for Jaffé-based sensors. Consequently, a perpendicular position of the paper-based device to the sample is recommended.

The stability of the sensors over an extended period of storage was also examined. The sensors were prepared according to the description provided in Materials and Methods section and then stored for 2 months in room temperature, 4 °C and -20 °C. The calibration curves were registered after that period and the fitting parameters were compared with the curves obtained for freshly prepared sensors. The results are displayed in Table S1. Storing the sensors in room temperature is not acceptable, because the linearity is not retained, whereas the storage in fridge (4 °C) or freezer (-20 °C) allows to maintain the linear response. However, it is important to point out that due to the logarithmic response of Jaffé-based sensors even a slight variation in the slope and intercept and a calibration curve would cause a significant error in the determined creatinine concentration if predefined calibration curve parameters were to be used. For that reason, Jaffé-based sensors are recommended to be prepared freshly, while DNBA-based sensors can be subjected to storage.

In the final step, the influence of urinary matrix components on the obtained results was established. In a recent study, we have compared the selectivity of the DNBA and Jaffé methods [5]. However, considering that the concentrations of the reagents as well as the target concentration of the analyte are now different, a similar interferences study was conducted. The results are presented in ESI, Table S2. The tested potential interferences do not result in a significant change in the response of the sensors for both methods therefore developed sensors can be successfully used for creatinine determination in undiluted urine.

### 3.5. Application user flow

An application for Android devices was written specifically for the purpose of user-friendly signal acquisition and processing. The user flow of the application is presented in Fig. 5. Firstly, the user is asked to choose the desired calculation method – either for DNBA-based sensors or Jaffé-based sensors and to set the a (slope) and b (intercept) parameters of the calibration curve. The selection of DNBA method allows for measurements with ISO 200 (Fig. 5, A) and a linear calibration characteristics whereas Jaffé method is set to take a photo with ISO 200 and to process the results with logarithmic dependence (Fig. 5, B). The user begins the measurement by pressing START button. The time between pressing start and capturing the picture is set to 5 s. Normally, this time should be the incubation time of the sensors, but to maintain versatility of the application it was kept shorter. During this time, the photo's preview is shown on the screen to ease a correct placement of the sensor. After the time passes, the taken photo is processed according to the algorithm described in section 2.6. The information available for the user is the full equation used to calculate the concentration of creatinine as well as RGB channel intensities (Fig. 5, C&D).

### 3.6. Real sensing scenarios

In the final stage of the project the usefulness of the developed sensors was confirmed by determining creatinine concentration in artificial urine samples. The photo capture and processing were accomplished in two ways: with OpenCamera application and ImageJ for processing and with the developed application for both purposes. In case of DNBA-based sensors the mentioned earlier washing out of the reagents effect was pronounced in urine samples, leading to significantly lowered results. This problem was solved by switching the placement of the reagents – the acidic solution was deposited in the sampling channel and sodium hydroxide in the detection zone. This is probably due to the fact that DNBA is readily soluble in alkaline solutions. In the original

**Table 3**

Statistical evaluation of obtained regressions and creatinine determination results in artificial urine samples. \*Values in brackets indicate critical values for the F and t tests at 95 % level of confidence.

<i>Jaffé-based sensors</i>						
Processing method	Manual processing with ImageJ			Automatic processing with the developed app		
Regression equation	$y = (-22.3 \pm 0.8) \log(x) + (53.5 \pm 0.6)$			$y = (-20.7 \pm 0.2) \log(x) + (47.3 \pm 0.2)$		
R <sup>2</sup>	0.991			0.999		
Statistical agreement of slopes*	F = 15.731 (7.146), t = 1.19 (2.31)					
Spiked concentration (mmol·L <sup>-1</sup> )	Found (mmol·L <sup>-1</sup> )	Recovery (%)	RSD (%)	Found (mmol·L <sup>-1</sup> )	Recovery (%)	RSD (%)
3.0	2.5	83	0.5	2.1	70	2.8
6.0	6.4	107	4.6	5.7	95	2.3
8.0	7.9	99	5.6	6.9	86	5.7
12	10.5	88	8.6	14	117	4.2
<i>DNBA-based sensors</i>						
Processing method	Manual processing with ImageJ			Automatic processing with the developed app		
Regression equation	$y = (-23.1 \pm 1.1) x + (235 \pm 4)$			$y = (-22.8 \pm 0.8) x + (230 \pm 3)$		
Correlation coefficient R <sup>2</sup>	0.986			0.993		
Statistical agreement of slopes*	F = 2.209 (7.146), t = 0.47 (2.23)					
Spiked concentration (mmol·L <sup>-1</sup> )	Found (mmol·L <sup>-1</sup> )	Recovery (%)	RSD (%)	Found (mmol·L <sup>-1</sup> )	Recovery (%)	RSD (%)
3.0	3.4	114	2.0	3.5	117	7.1
4.5	5.8	129	2.7	4.8	107	8.6
6.5	6.7	103	8.0	7.1	110	4.2
8.0	7.7	97	2.5	7.8	98	4.0

concept sample reaching the detection zone had alkaline pH, which caused dissolution of deposited DNBA and its displacement. Switching the placement of the reagents did not significantly affect the analytical parameters of the sensors but allowed for a uniform color formation in the detection zone. The spiked concentrations of the analyte are different for both kind of sensors due to different linear ranges of the methods. The obtained results are summarized in Table 3.

The calibration correlation registered with the developed application were statistically compared with those obtained with the traditional method. For Jaffé-based sensors the F-test showed a statistical difference between variances therefore a modified version of t-test for slopes comparison was used (according to equation 8 in Ref. [26]). The t-test proved statistical agreement between slopes of the calibration curves for both creatinine determination methods, demonstrating the analytical utility of the developed application compared to a well-established method of processing. As can be deduced from the obtained recoveries, the most accurate results can be achieved with DNBA method and automatic processing with the smartphone application.

#### 4. Conclusions

In this paper, a complete platform for point-of-care urinary creatinine quantification assisted with a smartphone has been reported. For the analytical procedure the only accessory required is a smartphone with installed app and equipped with a 3D-printed case. Two colorimetric creatinine detection methods were compared and DNBA-based sensors showed improved analytical parameters in comparison with Jaffé-based sensors. Besides a brief mention in Ref. [27], this is the first time DNBA method was used in paper-based sensors for the determination of creatinine.

It is important to highlight the versatility of the developed application – it can be successfully used to any kind of colorimetric or even fluorometric sensors provided that the photo taken is a colorful spot on a uniform background. The application provides similar analytical performance to routinely used in research camera application coupled with ImageJ software. A significant advantage of the developed application over the ones available in Google Play (like Color Picker or Color Grab) for similar purposes is the automatic detection of the zone of interest.

#### CRediT authorship contribution statement

**Izabela Lewińska:** Conceptualization, Methodology, Investigation, Formal analysis, Validation, Writing - original draft. **Mikołaj Speichert:** Methodology, Software, Writing - original draft. **Mateusz Granica:** Conceptualization, Resources, Writing - review & editing. **Łukasz Tymecki:** Writing - review & editing, Visualization, Supervision.

#### Declaration of Competing Interest

The authors declare that they have no known competing financial interests or personal relationships that could have appeared to influence the work reported in this paper.

#### Acknowledgement

This work was supported by statutory funds from Ministry of Education and Science, Poland (University of Warsaw).

#### Appendix A. Supplementary data

Supplementary material related to this article can be found, in the online version, at doi:<https://doi.org/10.1016/j.snb.2021.129915>.

#### References

- [1] C. Price, Point of care testing, *BMJ* 322 (2001) 1285–1288, <https://doi.org/10.1017/CBO9781139062381.018>.
- [2] A.W. Martinez, S.T. Phillips, M.J. Butte, G.M. Whitesides, Patterned paper as a platform for inexpensive, low-volume, portable bioassays, *Angew. Chemie - Int. Ed.* 46 (2007) 1318–1320, <https://doi.org/10.1002/anie.200603817>.
- [3] L.M. Fu, Y.N. Wang, Detection methods and applications of microfluidic paper-based analytical devices, *TrAC - Trends Anal. Chem.* 107 (2018) 196–211, <https://doi.org/10.1016/j.trac.2018.08.018>.
- [4] GBD Chronic Kidney Disease Collaboration, Global, regional, and national burden of chronic kidney disease, 1990–2017: a systematic analysis for the Global Burden of Disease Study 2017, *Lancet* 395 (2020) 709–733, [https://doi.org/10.1016/S0140-6736\(20\)30045-3](https://doi.org/10.1016/S0140-6736(20)30045-3).
- [5] I. Lewińska, Ł. Tymecki, M. Michalec, An alternative, single-point method for creatinine determination in urine samples with optoelectronic detector. Critical comparison to Jaffé method, *Talanta* 195 (2019) 865–869, <https://doi.org/10.1016/j.talanta.2018.12.003>.
- [6] J. Sittiwong, F. Unob, Paper-based platform for urinary creatinine detection, *Anal. Sci.* 32 (2016) 639–643, <https://doi.org/10.2116/analsci.32.639>.

- [7] E.L. Rossini, M.I. Milani, E. Carrilho, L. Pezza, H.R. Pezza, Simultaneous determination of renal function biomarkers in urine using a validated paper-based microfluidic analytical device, *Anal. Chim. Acta* 997 (2018) 16–23, <https://doi.org/10.1016/j.aca.2017.10.018>.
- [8] C.C. Tseng, R.J. Yang, W.J. Ju, L.M. Fu, Microfluidic paper-based platform for whole blood creatinine detection, *Chem. Eng. J.* 348 (2018) 117–124, <https://doi.org/10.1016/j.cej.2018.04.191>.
- [9] T.H. Chang, K.H. Tung, P.W. Gu, T.H. Yen, C.M. Cheng, Rapid simultaneous determination of paraquat and creatinine in human serum using a piece of paper, *Micromachines* 9 (2018), <https://doi.org/10.3390/mi9110586>.
- [10] K. Talalak, J. Noiphung, T. Songjaroen, O. Chailapakul, W. Laiwattanapaisal, A facile low-cost enzymatic paper-based assay for the determination of urine creatinine, *Talanta* 144 (2015) 915–921, <https://doi.org/10.1016/j.talanta.2015.07.040>.
- [11] S.H. Baek, C. Park, J. Jeon, S. Park, Three-dimensional paper-based microfluidic analysis device for simultaneous detection of multiple biomarkers with a smartphone, *Biosensors* 10 (2020), <https://doi.org/10.3390/bios10110187>.
- [12] F.H. Cincotto, E.L. Fava, F.C. Moraes, O. Fatibello-Filho, R.C. Faria, A new disposable microfluidic electrochemical paper-based device for the simultaneous determination of clinical biomarkers, *Talanta* 195 (2019) 62–68, <https://doi.org/10.1016/j.talanta.2018.11.022>.
- [13] E.L. Fava, T. Martimiano do Prado, T. Almeida Silva, F. Cruz de Moraes, R. Censi Faria, O. Fatibello-Filho, New disposable electrochemical paper-based microfluidic device with multiplexed electrodes for biomarkers determination in urine sample, *Electroanalysis* 32 (2020) 1075–1083, <https://doi.org/10.1002/elan.201900641>.
- [14] S. Boobphahom, N. Ruecha, N. Rodthongkum, O. Chailapakul, V.T. Remcho, A copper oxide-ionic liquid/reduced graphene oxide composite sensor enabled by digital dispensing: non-enzymatic paper-based microfluidic determination of creatinine in human blood serum, *Anal. Chim. Acta* 1083 (2019) 110–118, <https://doi.org/10.1016/j.aca.2019.07.029>.
- [15] A.K. Ellerbee, S.T. Phillips, A.C. Siegel, K.A. Mirica, A.W. Martinez, P. Striehl, N. Jain, M. Prentiss, G.M. Whitesides, Quantifying colorimetric assays in paper-based microfluidic devices by measuring the transmission of light through paper, *Anal. Chem.* 81 (2009) 8447–8452, <https://doi.org/10.1021/ac901307q>.
- [16] W.X. Kang, Q.Q. Yang, R.P. Liang, The comparative research on image segmentation algorithms, *First International Workshop on Education Technology and Computer Science* (2009) 703–707, <https://doi.org/10.1109/ETCS.2009.417>.
- [17] S. Zhou, Y. Zhao, J. Guan, J. Huang, A neighborhood-based clustering algorithm, *Proceedings of the 9th Pacific-Asia Conference on Advances in Knowledge Discovery and Data Mining* (2005) 361–371, [https://doi.org/10.1007/11430919\\_43](https://doi.org/10.1007/11430919_43).
- [18] T. Abe, Interaction of picric acid with sodium hydroxide in water, *Nature* 187 (1960) 234–235.
- [19] K. Cantrell, M.M. Erenas, I. De Orbe-Payá, L.F. Capitán-Vallvey, Use of the hue parameter of the hue, saturation, value color space as a quantitative analytical parameter for bitalonal optical sensors, *Anal. Chem.* 82 (2010) 531–542, <https://doi.org/10.1021/ac901753c>.
- [20] J. Il Hong, B.Y. Chang, Development of the smartphone-based colorimetry for multi-analyte sensing arrays, *Lab Chip* 14 (2014) 1725–1732, <https://doi.org/10.1039/c3lc51451j>.
- [21] E. Evans, E.F. Moreira Gabriel, W.K. Tomazelli Coltro, C.D. Garcia, Rational selection of substrates to improve color intensity and uniformity on microfluidic paper-based analytical devices, *Analyst* 139 (2014) 2127–2132, <https://doi.org/10.1039/c4an00230j>.
- [22] M. Jalali-Heravi, M. Arrastia, F.A. Gomez, How can chemometrics improve microfluidic research? *Anal. Chem.* 87 (2015) 3544–3555, <https://doi.org/10.1021/ac504863y>.
- [23] F.P. Wilson, D. Xie, A.H. Anderson, M.B. Leonard, P.P. Reese, P. Delafontaine, E. Horwitz, R. Kallem, S. Navaneethan, A. Ojo, A.C. Porter, J.H. Sondheimer, H. L. Sweeney, R.R. Townsend, H.I. Feldman, L.J. Appel, A.S. Go, J. He, J.W. Kusek, J. P. Lash, A. Ojo, M. Rahman, Urinary creatinine excretion, bioelectrical impedance analysis, and clinical outcomes in patients with CKD: the CRIC study, *Clin. J. Am. Soc. Nephrol.* 9 (2014) 2095–2103, <https://doi.org/10.2215/CJN.03790414>.
- [24] A. Mathaweesansurn, S. Thongrod, P. Khongkaew, C.M. Phechkrajang, P. Wilairat, N. Choengchan, Simple and fast fabrication of microfluidic paper-based analytical device by contact stamping for multiple-point standard addition assay: application to direct analysis of urinary creatinine, *Talanta* 210 (2020) 120675, <https://doi.org/10.1016/j.talanta.2019.120675>.
- [25] R. Hiraoka, K. Kuwahara, Y.C. Wen, T.H. Yen, Y. Hiruta, C.M. Cheng, D. Citterio, Paper-based device for naked eye urinary albumin/creatinine ratio evaluation, *ACS Sens.* 5 (2020) 1110–1118, <https://doi.org/10.1021/acssensors.0c00050>.
- [26] J.M. Andrade, M.G. Estévez-Pérez, Statistical comparison of the slopes of two regression lines: a tutorial, *Anal. Chim. Acta* 838 (2014) 1–12, <https://doi.org/10.1016/j.aca.2014.04.057>.
- [27] C. Heist, G. Bandara, D. Bemis, J. Pommerenck, V. Remcho, New paper-based microfluidic tools for the analysis of blood serum protein and creatinine built: via aerosolized deposition of polycaprolactone, *Anal. Methods* 10 (2018) 2994–3000, <https://doi.org/10.1039/c8ay00981c>.

**Izabela Lewińska** received her MSc degree from University of Warsaw in 2019. Her MSc thesis was devoted to fluorometric creatinine determination. Currently she is a PhD student and devotes her research to point-of-care creatinine sensing.

**Mikolaj Speichert** received his B.Eng. degree from Gdansk University of Technology in 2020. His thesis was devoted to real-time website focus maps creation based on users eye movements.

**Mateusz Granica** received his MSc degree from University of Warsaw in 2015. His MSc thesis was devoted to optical detection of urea. Currently he is a PhD student and his research is focused on microfluidic devices.

**Łukasz Tymecki** received his PhD (2005) and DSc (2016) from University of Warsaw. His scientific interests cover all aspects of miniaturization and mechanization of analytical methods.